

CN Neutrinos and the Sun's Primordial Core Metallicity

Wick Haxton

Institute for Nuclear Theory and Department of Physics
Box 351550, University of Washington, Seattle WA 98195

E-mail: haxton@phys.washington.edu

Abstract. I discuss the use of neutrinos from the CN cycle and pp chain to constrain the primordial solar core abundances of C and N at an interesting level of precision. A comparison of the Sun's deep interior and surface compositions would test a key assumption of the standard solar model (SSM), a homogeneous zero-age Sun. It would also provide a cross-check on recent photospheric abundance determinations that have altered the once excellent agreement between the SSM and helioseismology. Motivated by the discrepancy between convective-zone abundances and helioseismology, I discuss the possibility that a two-zone Sun could emerge from late-stage metal differentiation in the solar nebula connected with formation of the gaseous giant planets.

1. Introduction

One of the initial motivations for pursuing solar neutrino physics was to test our understanding of main-sequence stellar evolution and the Standard Solar Model (SSM). In the past two decades this goal was put aside, as difficulties in understanding the pattern of solar neutrino fluxes led to the discovery of solar neutrino oscillations. But because of the precision with which the relevant flavor physics is now known – and because the solar neutrino problem also spurred progress in the nuclear physics of the Sun and the development of high-statistics detectors such as Super-Kamiokande (SK) and SNO – the use of neutrinos as quantitative solar probe is now a practical possibility. Specifically, this talk summarizes recent arguments by Aldo Serenelli and me [1] that a measurement of the CN neutrino flux could test a key assumption of the SSM, the homogeneity of the zero-age main sequence Sun. This assumption, the basis for equating the SSM's primordial core metal abundances to today's surface metal abundances, may now be in some degree of conflict with observation: recent 3D modeling of photospheric absorption lines has led to a downward revision in the metal content of the solar convective zone [2], altering helioseismology in the upper radiative zone, where the temperature $\sim 2\text{--}5 \times 10^6$ K [3, 4, 5, 6]. In this region C, N, O, Ne, and Ar are partially ionized and particularly O and Ne have a significant influence on the radiative opacity.

A quantitative comparison between the Sun's surface and core abundances could prove useful in understanding the chemical evolution of other gaseous bodies in our solar system, whose interiors are not as readily probed. The Galileo and Cassini missions found significant metal enrichments in the H/He atmospheres of Jupiter and Saturn, e.g., abundances of C and N of \sim four times solar for Jupiter and $\sim 4\text{--}8$ for Saturn [7]. Planetary models that take account of these

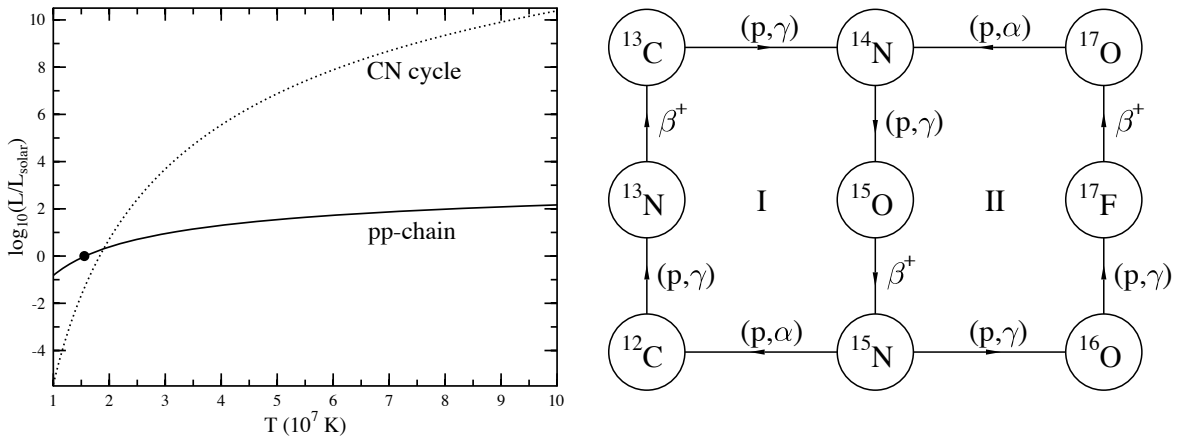


Figure 1. The right panel shows the CNO bi-cycle for hydrogen burning. The left compares the energy produced in the CN cycle with that produced in the pp-chain, as a function of temperature T_7 , measured in units of 10^7 K . The results are normalized to the pp-chain energy production at the Sun’s center and to solar metallicity, assuming equilibrium burning. The sharper CN-cycle dependence on temperature is apparent. If approximated as a power law T^x , x ranges between ~ 19 and ~ 22 over the range of temperatures typical of the Sun’s hydrogen-burning core. The dot marks the point corresponding to the Sun’s center, $T_7 \sim 1.57$.

data show that the gaseous giants are very significant solar-system metal reservoirs. The metal excess in these planets, estimated to be $\sim 40 - 90 M_{\oplus}$, is very similar to the depletion that would be needed in the convection zone to bring the photospheric abundances and helioseismology into agreement. Serenelli and I raised the possibility that a two-zone Sun resulted from a process in which the last $\sim 1\%$ of nebular gas was scoured of its metals by the process of planetary formation, then deposited on the early Sun to dilute the convective zone.

2. The CNO Bi-Cycle and its Neutrinos

The need for two mechanisms to burn hydrogen was recognized in the pioneering work of Bethe and collaborators. The first, the pp-chain, dominates energy production in our Sun and other low-mass main-sequence stars and can be considered a primary process in which the chain’s “catalysts,” deuterium, ^3He , and $^7\text{Be}/^7\text{Li}$ (the elements participating in the steps leading to ^4He), are synthesized as the chain burns to equilibrium.

But the sharper temperature dependence of a second mechanism, the CNO bi-cycle, is needed to account for the structure of more massive main-sequence stars. Unlike the pp-chain, the CNO bi-cycle (Fig. 1) is a secondary process: the catalysts for H burning are the pre-existing metals. Thus the CNO contribution to energy generation is proportional to stellar metallicity. The CN-cycle, denoted by I in Fig. 1, operates in the Sun. The cycle conserves the number abundance, but alters the distribution of metals as it burns into equilibrium, eventually achieving equilibrium abundances proportional to the inverses of the respective rates.

While responsible for only $\sim 1\%$ of solar energy generation, the CN cycle produces measurable neutrino fluxes. The slowest, rate-controlling reactions in the CN cycle are $^{14}\text{N}(p, \gamma)$ and $^{12}\text{C}(p, \gamma)$. The latter has reached equilibrium over most of the solar core. In fact, the rapid burning of ^{12}C , as the cycle seeks equilibrium at the start of the main sequence, likely drives convective mixing of the early solar core for $\sim 10^8 \text{ y}$. In contrast, the ^{14}N lifetime is shorter

than the age of the Sun only in regions where $T_7 \gtrsim 1.33$, which corresponds to $R \lesssim 0.1R_\odot$ in today's Sun, or equivalently the central 7% of the Sun by mass. Consequently, over a significant portion of the outer core, ^{12}C has been converted to ^{14}N , but further reactions are inhibited by the $^{14}\text{N}(\text{p},\gamma)$ bottleneck.

The BSP08(GS) SSM [8] – which employs recent updates of metal abundances and of the $^{14}\text{N}(\text{p},\gamma)$ S-factor – finds a modest CN-cycle contribution to solar energy generation of 0.8% and corresponding neutrino fluxes

$$^{13}\text{N}(\beta^+)^{13}\text{C} \quad E_\nu \lesssim 1.199 \text{ MeV} \quad \phi = (2.93_{-0.82}^{+0.91}) \times 10^8 / \text{cm}^2 \text{s}$$

$$^{15}\text{O}(\beta^+)^{15}\text{N} \quad E_\nu \lesssim 1.732 \text{ MeV} \quad \phi = (2.20_{-0.63}^{+0.73}) \times 10^8 / \text{cm}^2 \text{s}.$$

The ranges reflect conservative abundance uncertainties as defined empirically in [9]. The first reaction is part of the path from ^{12}C to ^{14}N , while the latter follows $^{14}\text{N}(\text{p},\gamma)$. Thus neutrinos from ^{15}O β decay are produced in the central core: 95% of the flux comes from the CN-equilibrium region, described above. About 30% of the ^{13}N neutrinos come from outside this region, primarily because of the continued burning of primordial ^{12}C : this accounts for the somewhat higher flux of these neutrinos.

The SSM makes several reasonable assumptions, including local hydrostatic equilibrium (the balancing of the gravitational force against the gas pressure gradient), energy generation by proton burning, a homogeneous zero-age Sun, and boundary conditions imposed by the known mass, radius, and luminosity of the present Sun. It assumes no significant mass loss or accretion. The homogeneity assumption allows the primordial core metallicity to be fixed to today's surface abundances. Corrections for the effects of diffusion of He and the heavy elements over 4.57 b.y. of solar evolution are included, and generally been helpful in improving the agreement between SSM predictions and parameters probed in helioseismology.

The SSM postulate of a homogeneous zero-age Sun is based on the assumptions 1) that the early pre-main-sequence Sun passed through a fully convective, highly luminous Hayashi phase, mixing the Sun; and 2) that no chemical differentiation in the gas accreted onto the Sun occurred after this phase, when the Sun develops a radiative core distinct from the convective surface zone.

Solar surface abundances are known, determined from analyses of photospheric atomic and molecular spectral lines. Traditionally the associated atmospheric modeling has been done in one dimension, in a time-independent hydrostatic analysis that incorporates convection via mixing-length theory. But much improved 3D models of the solar atmosphere have been developed recently to treat the radiation-hydrodynamics and time dependence of this problem. This 3D analysis led to a revision in solar metallicity from the previous standard, $Z=0.0169$ [10], to $Z=0.0122$ [2], thus altering SSM predictions. Hereafter we denote these as the GS and AGS abundances, respectively.

The predictions of solar models that use the GS solar composition, the most up to date of which is the BPS08(GS) [8] but including also the BP00 [11], BP04 [12] and BS05(OP) [4] models, are in excellent agreement with helioseismology. But those computed with the revised abundances are in much poorer agreement, with discrepancies exceeding 1% in the region just below the convective zone ($R \sim 0.65 - 0.70R_\odot$). Associated properties of the SSM, such as the depth of the convective zone and the surface He abundance, are also now in conflict with helioseismology. As discussed in [13], the discrepancies are significantly above measurement and solar model uncertainties.

The reduced core opacity also lowers the SSM prediction of the temperature-dependent ^8B neutrino flux by about 20%: the predicted ^8B flux using the GS abundances and Opacity Project [14] opacities (model BPS08(GS)) is $5.95 \times 10^6 / \text{cm}^2 \text{s}$, which drops to $4.72 \times 10^6 / \text{cm}^2 \text{s}$ when AGS abundances are used (model BPS08(AGS)). These results can be compared to the ^8B

neutrino flux deduced from the NCD-phase SNO data set of $[5.54 \text{ }^{+0.33}_{-0.31} \text{ (stat) } ^{+0.36}_{-0.34} \text{ (sys)}] \times 10^6/\text{cm}^2\text{s}$ [15].

3. The Sun as a Calibrated Laboratory

It has been recognized for many years that a measurement of the CN-cycle solar neutrino flux would, in principle, determine the metallicity of this core zone, allowing a comparison with abundance determined from the solar atmosphere. In the past several years new developments have occurred that may make such a measurement practical:

- Accurate calibrations of the solar core temperature by SNO and SK;
- Tight constraints on the oscillation parameters and matter effects that determine the flavor content of the CN and ^8B neutrino fluxes;
- Recent measurements of the controlling reaction of the CN cycle, $^{14}\text{N}(\text{p},\gamma)$, that have significantly reduced the nuclear physics uncertainties affecting SSM predictions of CN-cycle fluxes; and
- New ideas for high-counting rate experiments that would be sensitive to CN-cycle neutrinos, and from which reliable terrestrial fluxes could be extracted.

The analysis of [1], which examined whether CN neutrino experiments could place a significant constraint on the solar core’s primordial metallicity, used previous SSM work in which the logarithmic partial derivatives $\alpha(i, j)$ for each neutrino flux ϕ_i are evaluated for the SSM input parameters β_j ,

$$\alpha(i, j) \equiv \frac{\partial \ln [\phi_i / \phi_i(0)]}{\partial \ln [\beta_j / \beta_j(0)]}, \quad (1)$$

where $\phi_i(0)$ and $\beta_j(0)$ denote the SSM best values. This information, in combination with the assigned uncertainties in the 19 β_j of the SSM, then provides an estimate of the uncertainty in the SSM prediction of ϕ_i . In particular, crucial to the current analysis is the dependence [9] on the mass fractions (measured relative to hydrogen) of different heavy elements,

$$\beta_j = \frac{\text{mass fraction of element } j}{\text{mass fraction of hydrogen}} \equiv X_j. \quad (2)$$

Having this information not as a function of the overall metallicity Z , but as a function of the individual abundances, allows one to separate the “environmental” effects of the metals in the solar core from the special role of primordial C and N as catalysts for the CN cycle. By environmental effects we mean the influence of the metals on the opacity and thus the ambient core temperature, which controls the rates of neutrino-producing reactions of both the pp-chain and CN cycle. In [1] the temperature-dependent ^8B neutrino flux was used to calibrate the environmental effects of the metals and of other SSM parameters, thus isolating the special CN-cycle dependence on primordial C+N. This primordial abundance can be expressed, with very little residual solar model uncertainty, in terms of the measured ^8B neutrino flux and nuclear cross sections that have been determined in the laboratory.

The partial derivatives allow one to define the power-law dependencies of neutrino fluxes, relative to the SSM best-value prediction $\phi_i(0)$

$$\phi_i = \phi_i(0) \prod_{j=1}^N \left[\frac{\beta_j}{\beta_j(0)} \right]^{\alpha(i, j)} \quad (3)$$

where the product extends over $N = 19$ SSM input parameters. This expression can be used to evaluate how SSM flux predictions will vary, relative to $\phi_i(0)$, as the β_j are varied. Alternatively,

the process can be inverted: a flux measurement could in principle be used to constrain an uncertain input parameter.

The baseline SSM calculation used in [1], BPS08(AGS) [8], employed the recently determined AGS abundances for the volatile elements C, N, O, Ne, and Ar, rather than the previous GS standard composition. It should be noted that AGS includes a downward revision by 0.05 dex of the Si photospheric abundance compared to GS and, accordingly, a similar reduction in the meteoritic abundances. The partial derivatives needed in the present calculation are summarized in Tables 1 (solar model parameters and nuclear cross sections) and 2 (abundances).

The SSM estimate of uncertainties in the various solar neutrino fluxes ϕ_i can be obtained by folding the partial derivatives with the uncertainties in the underlying β_j . In particular, it is convenient to decompose Eq. (3) into its dependence on solar parameters and non-CN metals, nuclear S-factors, and the primordial C and N abundances,

$$\phi_i = \phi_i^{SSM} \prod_{j \in \{\text{Solar and Metals} \neq \text{C,N}\}} \left[\frac{\beta_j}{\beta_j(0)} \right]^{\alpha(i,j)} \prod_{j \in \{\text{Nuclear}\}} \left[\frac{\beta_j}{\beta_j(0)} \right]^{\alpha(i,j)} \prod_{j \in \{\text{C,N}\}} \left[\frac{\beta_j}{\beta_j(0)} \right]^{\alpha(i,j)} \quad (4)$$

where the first term will be designated the “environmental” uncertainty – SSM solar parameters and metal abundances that primarily influence neutrino flux predictions through changes they induce in the core temperature. These are, respectively, the uncertainties in the photon luminosity L_\odot , the mean radiative opacity, the solar age, and calculated He and metal diffusion; and the fractional abundances of O, Ne, Mg, Si, S, Ar, and Fe. The estimated 1σ fractional uncertainties for these parameters are given in [1]. The abundances of Mg, Si, S, and Fe are meteoritic, while those of the volatile elements C, N, O, Ne, and Ar are photospheric.

The next term contains the effects of nuclear cross section uncertainties on flux predictions. The β_j are the S-factors for p+p (S_{11}), $^3\text{He} + ^3\text{He}$ (S_{33}), $^3\text{He} + ^4\text{He}$ (S_{34}), p + ^7Be (S_{17}), e + ^7Be (S_{e7}), and p + ^{14}N (S_{114}). The estimated 1σ fractional uncertainties are also given in [1].

The last term is the contribution of the primordial C and N abundances. As Table 2 shows, pp-chain neutrino fluxes are relatively insensitive to variations in these abundances, as the heavier nuclei like Fe have a more important influence on the core opacity. But the expected, nearly linear response of the ^{13}N and ^{15}O neutrino fluxes to these abundances is apparent. These are the abundances we would like to constrain by a future measurement of the ^{13}N and ^{15}O solar neutrino fluxes. Such a measurement begins to be of interest if these abundances could be determined with an accuracy significantly better than 30%.

Were one to vary the 11 SSM parameters designated as “environmental” according to their assigned uncertainties (taking them to be uncorrelated), a 7.5% SSM net uncertainty in $\phi(^{13}\text{N})$ would be obtained. This uncertainty would be one of dominant ones in the analysis of present interest. But, as discussed in [1] in more detail, these environmental uncertainties influence neutrino fluxes through their impact on the core temperature, regardless of the details of which parameters are varied. Consequently, there are strong environmental correlations between different neutrino fluxes, allowing one to form ratios of fluxes that are much less sensitive to environmental effects. Furthermore these correlations remain valid for parameter variations far outside accepted SSM uncertainties.

This is illustrated in the SSM Monte Carlo tests represented in Fig. 3. One finds that a flux ratio such as

$$\frac{\phi(^{15}\text{O})}{\phi(^{8}\text{B})^K}, \quad (5)$$

where the exponent $K \sim 0.828$ is taken from the fit shown in Fig. 3, is much less sensitive to environmental uncertainties than either the numerator or denominator separately. This is apparent from the entries in Tables 1 and 2. As $\phi(^{8}\text{B})$ can be taken from SK and SNO measurements, most of the environmental uncertainty in predicting $\phi(^{15}\text{O})$ can be eliminated.

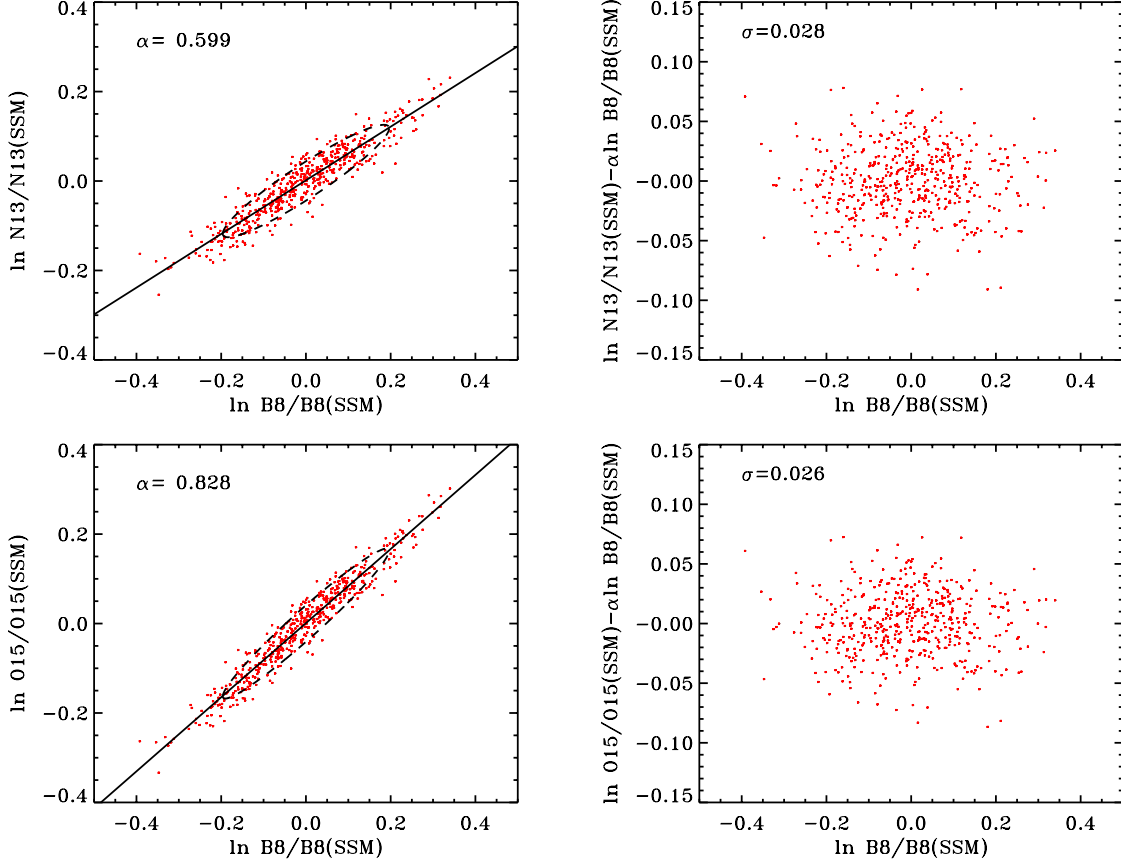


Figure 2. Results from SSM Monte Carlo simulations in which the 11 environmental parameters (see text) have been varied. The two left panels show the correlations between the ^8B flux and the two CN-cycle neutrino fluxes ^{13}N and ^{15}O . The slopes of the correlations are given in the plots, together with the 68.3% confidence level contours. The panels on the right show the residuals from the fits, 2.8% and 2.6% for the ^{13}N and ^{15}O fluxes respectively – the residual environmental uncertainty that remains after making use of the ^8B flux constraint.

Effectively, $\phi(^8\text{B})$ becomes a “thermometer” constraining core temperature changes induced by varying the environmental β_j . In this way one obtains a more precise relationship between the CN flux, a quantity that should be measured quite accurately in next-generation experiments like SNO+, and the core abundances of C and N.

4. The Analysis for Elastic Scattering and Neutrino Oscillations

The analysis requires a number of steps that will be summarized here, as more detail can be found in Ref. [1]. The total ^8B flux (the instantaneous solar flux), normalized to the SSM best value, can be related to rates that would be measured in terrestrial detectors by

$$\frac{\phi(^8\text{B})}{\phi^{SSM}(^8\text{B})} = \frac{\phi(^8\text{B})\langle\sigma^{SK}(^8\text{B}, \delta m_{12}^2, \theta_{12})\rangle}{\phi^{SSM}(^8\text{B})\langle\sigma^{SK}(^8\text{B}, \delta m_{12}^2, \theta_{12})\rangle} \equiv \frac{R_{exp}^{SK}(^8\text{B})}{R_{cal}^{SK}(^8\text{B}, \delta m_{12}^2, \theta_{12})} \quad (6)$$

Table 1. Partial derivatives $\alpha(i, j)$ of neutrino fluxes with respect to solar environmental and nuclear cross section parameters.

Source	Environmental β_j				Nuclear β_j					
	L_\odot	Opacity	Age	Diff.	S_{11}	S_{33}	S_{34}	S_{17}	S_{e7}	S_{114}
$\phi(^8\text{B})$	7.16	2.70	1.38	0.28	-2.73	-0.43	0.85	1.0	-1.0	-0.020
$\phi(^{13}\text{N})$	4.40	1.43	0.86	0.34	-2.09	0.025	-0.053	0.0	0.0	0.71
$\phi(^{13}\text{N})/\phi(^8\text{B})^{0.599}$	0.11	-0.19	0.03	0.17	-0.45	0.28	-0.56	-0.60	0.60	0.72
$\phi(^{15}\text{O})$	6.00	2.06	1.34	0.39	-2.95	0.018	-0.041	0.0	0.0	1.00
$\phi(^{15}\text{O})/\phi(^8\text{B})^{0.828}$	0.07	-0.18	0.20	0.16	-0.69	0.37	-0.74	-0.83	0.83	1.02

Table 2. Partial derivatives $\alpha(i, j)$ of neutrino fluxes with respect to fractional abundances of the primordial heavy elements.

Source	C, N β_j		Environment Abundance β_j						
	C	N	O	Ne	Mg	Si	S	Ar	Fe
$\phi(^8\text{B})$	0.027	0.001	0.107	0.071	0.112	0.210	0.145	0.017	0.520
$\phi(^{13}\text{N})$	0.874	0.142	0.044	0.030	0.054	0.110	0.080	0.010	0.268
$\phi(^{13}\text{N})/\phi(^8\text{B})^{0.599}$	0.858	0.141	-0.020	-0.013	-0.013	-0.016	-0.007	0.000	-0.043
$\phi(^{15}\text{O})$	0.827	0.200	0.071	0.047	0.080	0.158	0.113	0.013	0.393
$\phi(^{15}\text{O})/\phi(^8\text{B})^{0.828}$	0.805	0.199	-0.018	-0.012	-0.013	-0.016	-0.007	-0.001	-0.038

Here $\langle\sigma^{SK}\rangle$ is an effective cross section that takes into account all of the neutrino flavor and detector response issues (trigger efficiencies, resolution, cross section uncertainties, oscillations, etc.) that determine the relationship between a measured detector rate and the instantaneous solar flux. The numerator of the ratio on the right is a directly measured experimental quantity: the SK elastic scattering rate for producing recoil electrons with apparent energies between 5.0 and 20 MeV, per target electron per second. The denominator is a theoretical quantity, computed by folding the SSM best-value ^8B flux produced in the Sun with the cross section for (ν_e, e) elastic scattering, averaged over a normalized ^8B spectrum, defined for the specific experimental conditions of SK, and including the effects of flavor mixing that alter the flux during transit from the Sun to the detector. This cross section is calculated from laboratory measurements of detector properties, the β decay spectrum, the underlying neutrino-electron cross sections, and most critically, the parameters governing oscillations. We describe these factors below.

The experimental rate comes from the 1496 days of measurements of SK I [16]. From the SK I rate/kiloton/year

$$520.1 \pm 5.3(\text{stat}) \pm_{-16.6}^{+18.2}(\text{sys}) \text{ kton}^{-1} \text{ y}^{-1}. \quad (7)$$

we find $R_{exp}^{SK}(^8\text{B})$,

$$4.935 \pm 0.05(\text{stat}) \pm_{-0.16}^{+0.17}(\text{sys}) \times 10^{-38} \text{ electron}^{-1} \text{ s}^{-1} \quad (8)$$

(or ~ 0.049 Solar Neutrino Units, or SNU). The dominant systematic error includes estimates for the energy scale and resolution, trigger efficiency, reduction, spallation dead time, the gamma ray cut, vertex shift, background shape for signal reduction, angular resolution, and lifetime uncertainties. The combined statistical and systematic error is $\sim \pm 3.6\%$.

To evaluate the denominator in Eq. (6) we need the suitably averaged cross section, defined for the window used by the SK I collaboration,

$$\langle\sigma^{SK}(^8\text{B}, \delta m_{12}^2, \theta_{12})\rangle = \int dE_\nu \phi_{norm}^{^8\text{B}}(E_\nu) \left[P_{\nu_e}(E_\nu, \delta m_{12}^2, \sin^2 2\theta_{12}) \int_{T=0}^{T^{max}(E_\nu)} dT \sigma_{\nu_e}^{es}(T) \right]$$

$$+ P_{\nu_\mu}(E_\nu, \delta m_{12}^2, \sin^2 2\theta_{12}) \int_{T=0}^{T^{max}(E_\nu)} dT \sigma_{\nu_\mu}^{es}(T) \left] \int_{5 \text{ MeV}}^{20 \text{ MeV}} d\epsilon_a f_{\text{trig}}(\epsilon_a) \rho(\epsilon_a, \epsilon_t = T + m_e) \right] \quad (9)$$

where $\phi_{norm}^{8B}(E_\nu)$ is the normalized 8B neutrino spectrum. Equation (9) involves an integral over the product of this spectrum and the energy-dependent oscillation probabilities. ($P_{\nu_e} + P_{\nu_\mu} = 1$, assuming oscillations into active flavors. P_{ν_μ} can be defined as the oscillation probability to heavy flavors, if the effects of three flavors are considered.) A given E_ν fixes the range of kinetic energies T of the scattered electron, over which an integration is done; in the laboratory frame $T^{max} = 2E_\nu^2/(m_e + 2E_\nu)$. The integrand includes the elastic scattering cross sections $\sigma^{es}(T)$ for electron and heavy-flavor neutrinos and the SK resolution function $\rho(\epsilon_a, \epsilon_t)$, where $\epsilon_t = T + m_e$ is the true total electron energy while ϵ_a is apparent energy, as deduced from the number of phototube hits in the detector. Finally, an integral must be done over the window used by the experimentalists, apparent electron energies ϵ_a between 5 and 20 MeV. The deduced counting rate includes the triggering probability that a event of apparent energy ϵ_a will be recorded in the detector. Resolution and triggering functions for SK are given in [1].

Similarly, the CN-cycle neutrino response for a detector like SNO+ is

$$\frac{\phi(^{15}\text{O})}{\phi^{SSM}(^{15}\text{O})} \equiv \frac{R_{exp}^{B/S}(^{15}\text{O})}{R_{cal}^{B/S}(^{15}\text{O}, \delta m_{12}^2, \theta_{12})} = \frac{R_{exp}^{B/S}(\text{CN})/(1 + \alpha(0.8, 1.3))}{R_{cal}^{B/S}(^{15}\text{O}, \delta m_{12}^2, \theta_{12})} \quad (10)$$

where the experimental rate for ^{15}O neutrinos has been written in terms of the total CN-neutrino rate $R_{exp}^{B/S}(\text{CN})$ by introducing a correction factor $\alpha \sim 0.12$ that accounts for the ^{13}N neutrino contribution. As discussed in [1], α can be measured in principle, but can also be evaluated from theory, with negligible uncertainty. No measurement of $R_{exp}^{B/S}(\text{CN})$ currently exists, of course. But such measurements could be made in Borexino or SNO+, existing or planned detectors using large volumes of organic scintillator and placed quite deep underground. A window for the apparent kinetic energy T of the scattered electron of 0.8-1.3 MeV has been discussed by the Borexino group. As the ^7Be 0.866 MeV line corresponds to $T^{max} \sim 0.668$ MeV, this window would limit contamination from ^7Be neutrino recoil electrons.

As discussed in [1], one can use Eqs. (6) and (10) in expressions based on Eq. (4), then on dividing obtain

$$\begin{aligned} \frac{R_{exp}^{B/S}(\text{CN})}{R_{cal}^{B/S}(^{15}\text{O}, \delta m_{12}^2, \theta_{12})} &= (1.120 \pm 0.003) \left[\frac{R_{exp}^{SK}(^8\text{B})}{R_{cal}^{SK}(^8\text{B}, \delta m_{12}^2, \theta_{12})} \right]^{0.828} \\ &\times [1 \pm 2.6\%(\text{resid. envir.}) \pm 7.6\%(\text{nuclear})] \left(\frac{X(^{12}\text{C})}{X(^{12}\text{C})_{SSM}} \right)^{0.805} \left(\frac{X(^{14}\text{N})}{X(^{14}\text{N})_{SSM}} \right)^{0.199}. \end{aligned} \quad (11)$$

Effectively the SK rate has been used to limit SSM “environmental” uncertainties, leaving an error budget dominated by the nuclear physics. But this source of error is under laboratory control and will be reduced as nuclear reaction measurements continue. The last two terms are the primordial abundances one would like to constrain. The role of the SSM in this equation is to define a set of parameters and thus a set of reference rates, about which we then explore possible variations. Those variations generate the environmental and nuclear uncertainties discussed above.

The R_{cal} factors in Eq. (11) contain additional uncertainties discussed in [1], including one important one, that associated with neutrino oscillations. Apart from the dependence on the solar density profile, this should be considered a laboratory uncertainty, analogous to nuclear cross sections. Uncertainties in oscillation parameters will continue to be refined by astrophysical, accelerator and reactor measurements.

The LMA parameter uncertainties in SK and Borexino/SNO+ are anti-correlated. Most of the low-energy ^{15}N neutrinos do not experience a level crossing, residing instead in a portion of the MSW plane where the oscillations are close to the vacuum oscillation limit,

$$P_{\nu_e}(E_\nu) \rightarrow 1 - \frac{1}{2} \sin 2\theta_{12}, \quad (12)$$

so that an increase in the vacuum mixing angle θ_{12} decreases the ν_e survival probability. The higher energy ^8B neutrinos are largely within the MSW triangle, described by an adiabatic level crossing. The limiting behavior for an adiabatic crossing is

$$P_{\nu_e}(E_\nu) \rightarrow \frac{1}{2}(1 - \cos 2\theta_{12}) \quad (13)$$

so that an increase in θ_{12} increases the survival probability. This anti-correlation thus leads to larger effects in the ratio.

The impact of this uncertainty on Eq. (11) was analyzed in [1], using the allowed regions for θ_{12} and δm_{12}^2 obtained in KamLAND's combined analysis, yielding

$$\frac{R_{cal}^{B/S}(^{15}\text{O}, \delta m_{12}^2, \theta_{12})}{R_{cal}^{SK}(^8\text{B}, \delta m_{12}^2, \theta_{12})^{0.825}} = (1 \pm 0.049) \left[\frac{R_{cal}^{B/S}(^{15}\text{O}, \delta m_{12}^2, \theta_{12})}{R_{cal}^{SK}(^8\text{B}, \delta m_{12}^2, \theta_{12})^{0.825}} \right]^{BV} \quad (14)$$

where BV denotes the SSM best-value ratio.

Thus the overall uncertainty budget in Eq. (11) includes the experimental uncertainty of the SK “thermometer” of 3%, residual solar environmental uncertainties at 2.6%, LMA parameter uncertainties at 4.9%, and nuclear S-factor uncertainties of 7.6%. The overall uncertainty in the “theoretical” relationship between a future SNO+ or Borexino CN-neutrino flux and core C/N metals is thus about 9.6%. As the nuclear physics uncertainty dominates, one would expect this relationship to become more precise when ongoing analyses of data obtained by the LUNA collaboration and others for $^{14}\text{N}(p, \gamma)$ are completed. An appropriate goal would be 3.5% in this S-factor, a 30% improvement. The uncertainty in $^{14}\text{N}(p, \gamma)$ would no longer dominate the nuclear physics error budget, but instead would be comparable to the contributions from S_{33} and S_{34} . However, the current 9.6% uncertainty is not a bad starting point, as first-generation CN-cycle neutrino experiments are expected to measure this flux to an accuracy of about 10%. That is, the theoretical uncertainty will not dominate the experimental uncertainty, even without anticipated nuclear physics improvements.

5. Future Experiments and Summary

The work reported here was motivated in part by new detectors that might enable a high-statistics measurement of the CN-cycle neutrinos. Two possibilities are Borexino and SNO+, detectors based on ultra-clean organic scintillation liquids. Borexino, which operates within Gran Sasso, must deal with a serious background, cosmogenic ^{11}C (a β^+ source). The collaboration has discussed a possible triple-coincidence veto [17] to limit this background.

Because of SNOlab's 6.0 km.w.e. depth, ^{11}C will be much less troublesome in SNO+, an experiment that will use the SNO cavity and about three times more scintillator than Borexino. Figure 3 shows a simulation of the expected SNO+ response, performed by the experimenters (Chen, private communication). (Note that the simulation is based on the BS05(OP) SSM and the best-fit LMA solution to the solar neutrino problem, rather than the updated BPS08(AGS) used in this paper.) The CN-neutrino event rate for an energy window above 0.8 MeV was found to be 2300 counts/year. The experimenters concluded that SNO+ could determine the CN-neutrino rate to an accuracy of approximately 10%, after three years of running [18]. This

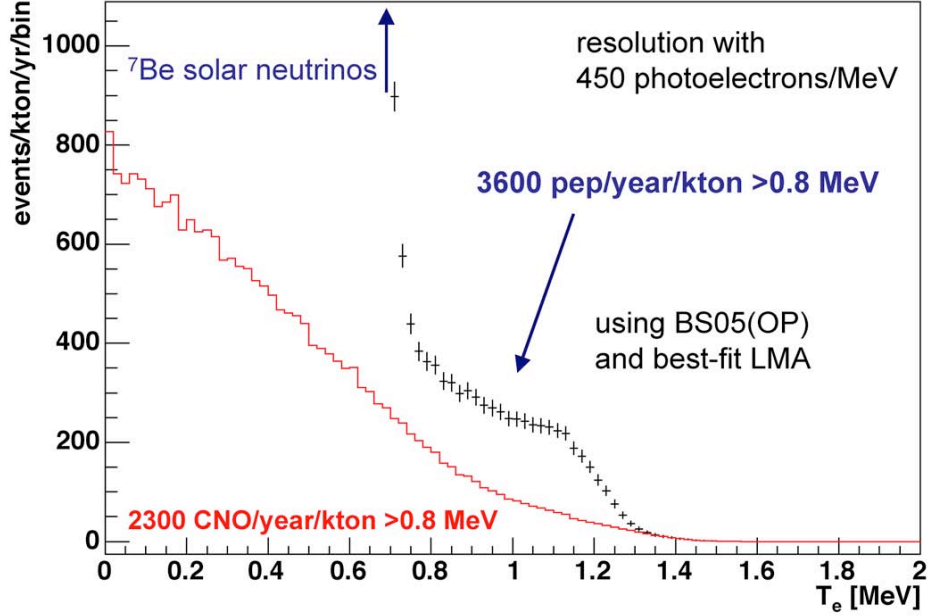


Figure 3. A simulation of the ${}^7\text{Be}$, pep, and CNO electron recoil spectrum expected in SNO+. This figure is due to M. C. Chen [18].

is an appropriate goal for such a first-generation CN-cycle neutrino measurement, as it would approach the accuracy with which that flux could be related theoretically to the Sun’s primordial core C and N abundances, as argued in this paper.

One main point of this talk is that if a 10% measurement can be made, an analysis could be done that limits theoretical uncertainties to below this level, provided one uses SK as a thermometer to eliminate environmental uncertainties. Indeed, both of the limiting errors in such an analysis can be addressed in future laboratory measurements, namely nuclear cross sections ($\sim 7.6\%$) and LMA oscillation parameters ($\sim 4.9\%$). One goal should be the reduction of these error bars to the level of uncertainty of the SK thermometer, $\sim 3\%$.

In my view, the primary motivation for such a measurement is to test the SSM assumption of a homogeneous zero-age-main-sequence Sun, given recent revisions of metal abundances derived from analyses of photospheric absorption lines. One could try to reconcile helioseismology with lower photospheric metal abundances by violating this SSM assumption, adopting a two-zone Sun with a low-Z convective zone.

It is intriguing that a possible mechanism for diluting the convective zone exists. The solar system’s primary reservoir for metals, the gaseous giant planets, formed late in the evolution of the solar nebula, incorporating an excess of metal estimated at $40\text{--}90\,M_{\oplus}$. This mass is similar to the deficit of metals in the convective zone, were one to interpret the helioseismology/photospheric abundance discrepancy in the most naive way. This raises a provocative question: is it possible that the process that concentrated metals in the gaseous giants also produced a large volume of metal-depleted gas that subsequently was accreted onto the Sun’s surface? If so, late-stage accretion of depleted gas onto the Sun would have not only diluted the convective zone, but generated a transition zone in the modern Sun’s upper radiative zone – one that might alter helioseismology in that region. One would also expect abundance anticorrelations between the atmospheres of the Sun and gaseous giants. While the suggestion of a common chemical mechanism linking the convection zone and the gaseous giants is speculative,

it provides additional motivation for exploiting the CN neutrinos as a quantitative probe of solar core metallicity.

6. Acknowledgments

This work was supported in part by the Office of Nuclear Physics, US Department of Energy, under grant DE-FG02-00ER-41132.

References

- [1] Haxton W C and Serenelli A M 2008, to appear in *Ap. J.*
- [2] Asplund M, Grevesse N, and Sauval A J 2005 in *Cosmic Abundances as Records of Stellar Evolution and Nucleosynthesis* vol 336, ed T G Barnes III and F N Bash (Astronomical Society of the Pacific) p 25
- [3] Bahcall J N, Basu S, Pinsonneault M, and Serenelli A M 2005 *Ap. J.* **618** 1049
- [4] Bahcall J N, Serenelli A M, and Basu S 2005 *Ap. J.* **621** L85
- [5] Antia H M and Basu S 2005 *Ap. J.* **620** L129
- [6] Montalbán J, Miglio A, Noels A, Grevesse N, and di Mauro, M P 2004 in *SOHO 14 Helio- and Asteroseismology: Towards a Golden Future* vol 559, ed D Danesy (ESA Special Publication) p 574
- [7] Guillot, T 2005 *Annual Review of Earth and Planetary Sciences* **33** 493
- [8] Peña-Garay C and Serenelli A M 2008, in preparation
- [9] Bahcall J N and Serenelli A M 2005 *Ap J* **626** 530
- [10] Grevesse N and Sauval A J 1998 *Space Science Reviews* **85** 161
- [11] Bahcall J N, Pinsonneault M H, and Basu S 2001 *Ap J* **555** 990
- [12] Bahcall J N and Pinsonneault M H 2004 *Phys. Rev. Lett.* **92** 121301
- [13] Bahcall J N, Serenelli A M, and Basu S 2006, *Ap. J. Suppl.* **165** 400
- [14] Badnell N R et al. 2005 *MNRAS* **360** 458
- [15] SNO Collaboration 2008 to appear in *Phys. Rev. Lett.* (arXiv:0806.0989)
- [16] Hosaka J, et al. 2006 *Phys. Rev. D* **73** 112001
- [17] The BOREXINO Collaboration 2005 *Nucl. Phys. B Proc. Suppl.* **145** 29
- [18] Chen, M C 2007 in *Next Generation Nucleon Decay and Neutrino Dectectors*, vol 944, ed J R Wilkes (AIP) p 25